Talanta 103 (2013) 14–19

Contents lists available at SciVerse ScienceDirect

Talanta

journal homepage: www.elsevier.com/locate/talanta

Highly sensitive ochratoxin A impedimetric aptasensor based on the immobilization of azido-aptamer onto electrografted binary film via click chemistry

Akhtar Hayat [a], Audrey Sassolas [a], Jean-Louis Marty [a,*], Abd-Elgawad Radi [b]

[a] BIOMEM, Université de Perpignan, 52 Avenue Paul Alduy, 66860 Perpignan Cedex, France
[b] Department of Chemistry, Faculty of Science, Mansoura University, 34517 Dumyat, Egypt

ARTICLE INFO

Article history:
Received 8 August 2012
Received in revised form
16 September 2012
Accepted 22 September 2012
Available online 4 October 2012

Keywords:
Click chemistry
Azido-aptamer
Impedimetric aptasensor
Ochratoxine A
Beer sample

ABSTRACT

The aptamer immbolization onto organized mixed layers of diazonium salts via click chemistry was explored. The immobilized aptamer was employed in the fabrication of a highly sensitive and reusable electrochemical impedimetric aptasensor for the detection of ochratoxin A (OTA). The screen-printed carbon electrodes (SPCEs) were first modified by electrografting of a protected 4-((trimethylsilyl)ethynyl) benzene (TMSi-Eth-Ar) layer followed by a second one of *p*-nitrobenzene (*p*-NO_2-Ar) by means of electrochemical reduction of their corresponding diazonium salts, (TMSi-Eth-Ar-N_2^+) and (*p*-NO_2-ArN_2^+). After deprotection, a layer with active ethynyl groups was obtained. In the presence of copper (I) catalyst, the ethynyl groups reacted efficiently with aptamer bearing an azide function, thus forming a covalent 1,2,3-triazole linkage. Cyclic voltammetry (CV) and electrochemical impedance spectroscopy (EIS) in the presence of ferri/ferrocyanide redox probe $[Fe(CN)_6]^{4-/3-}$ were used to characterize each step in the aptasensor development. The increase in electron-transfer resistance (R_{et}) values due to the specific aptamer–OTA interaction was proportional to the concentration of OTA in a range between 1.25 ng/L and 500 ng/L, with a detection limit of 0.25 ng/L.

1. Introduction

Aptamers are nucleic acid ligands which are isolated from random-sequence DNA pools by a technique known as SELEX (systematic evolution of ligands by exponential enrichment) or *in vitro* selection [1]. Aptamers are capable of binding tightly and specifically to targets ranging from small molecules to complex multimeric structures [2,3]. Aptamers were used as affinity ligands instead of monoclonal and polyclonal antibodies, as a promising alternative for many target molecules [4,5]. Up to now, most of the developed aptasensors are based on optical and electrochemical transduction methods. Electrochemical aptasensors have been appeared as promising bio-tool due to their low limit of detection and high sensitivity. In order to increase the system sensitivity, many electrochemical aptasensors are fabricated by labeling the aptamers with electroactive materials such as enzyme, ferrocene and methylene blue [6–8]. However, the labeling of aptamer makes the assays more complex, time consuming and laborious. Moreover, labeling process affects the binding affinity between the targets and their aptamers to a certain degree [9,10]. In an effort to overcome these drawbacks, it is important to develop label free and highly sensitive electrochemical aptasensors. Among the label free methods, electrochemical impedance spectroscopy (EIS) has attained growing attention because of high sensitivity, low cost, fast response time and simple equipment. It has been proven that EIS can be successfully used as an enzyme sensor [11], immunosensor [12] and DNA sensor [13]. In the present work, a label free impedimetric aptasensor based on the immobilization of azido-aptamer onto binary film via click chemistry was explored to detect ochratoxin A (OTA). The electrochemical grafting of binary film and click chemistry employed here were expected to provide uniform, controlled and efficient immobilization of aptamer to improve the sensitivity of the system, in addition to reducing the non-specific signal.

Click chemistry is attracting lot of interest and importance in recent years [14,15]. As an azide/alkyne 1,3-dipolar cycloaddition, it was first introduced by Huishgen in 1984 as a reaction at high temperature in organic solvent [16]. In 2001, Sharpless et al. performed this reaction in aqueous phase with Cu (1) as catalyst under very mild conditions [17]. From then on, click chemistry received vital importance not only because it is irreversible, quantitative and mildly processed, but also because the 1,2,3-triazole ring formed in the reaction is similar to peptide bond in atom placement and electronic properties. The ring like peptide

* Corresponding author. Tel.: +33 468 66 22 54; fax: +33 468 66 22 23.
E-mail address: jlmarty@univ-perp.fr (J.-L. Marty).

0039-9140/$ - see front matter © 2012 Elsevier B.V. All rights reserved.
http://dx.doi.org/10.1016/j.talanta.2012.09.048

helps to maintain biological activity of the immobilized biomolecule [18,19]. Moreover, this heterogeneous coupling reaction is fast, resistant to side reactions, selective, compatible to various solvents (including water), reproducible, highly tolerant to reaction conditions and has high yield. Additionally, the formed 1,4-disubsituted 1,2,3-triazole is very stable under physiological conditions, and the azides are highly energetic and inert to biomolecules, which is useful for site-specific immobilization of biomolecules onto solid surface [20]. These advantages make click chemistry suitable for electrochemical grafting of biomolecules onto electrode surface. Although covalent attachment based on click chemistry for enzymes [21,22] and proteins [14] was performed, the concept of click chemistry for aptamer immobilization is new, and not reported in the literature.

Similarly, potential and interesting applications can be obtained only when biomolecules are properly immobilized on solid surface. Recently, the direct and covalent immbolization of biomolecules have been used to functionalize solid interface, such as carbon, silicon, metals, and diamonds [23]. However, covalent immobilization is difficult to control and yields randomly bound biomolecule with poor orientation or inappropriate alignment, which results in inefficient electron transfer to electrode surface [21]. An alternative strategy was recently developed by Leroux et al., who successfully used a binary layer containing two reagents to obtain the uniform, compact and controlled modified electrode surface [24]. On the basis of this concept, we explored here the use of two binary films of diazonium salts in the construction of aptasensor. It was expected that the controlled and uniform modified electrode surface would provide the systematic immobilization of aptamer, to improve the system reproducibility and sensitivity. It is worth to note that the concept of click chemistry and electrode surface modification with binary films is reported for the first time in the construction of aptasensor.

Ochratoxin A was selected as target molecule for this study because it contaminates a variety of food commodities. OTA has several toxicological effects such as nephrotoxic, hepatotoxic, neurotoxic, teratogenic and immunotoxic and it is believed to cause increased oxidative stress at a cellular level [25,26]. The European Union has introduced some regulatory limits to control the level of OTA in food stuff such as raw cereal grains (5 μg/kg), dried fruits (10 μg/kg), roasted coffee and coffee products (5 μg/kg), grape juice (2 μg/kg) (EC No. 123/2005) and also for all types of wines (2 μg/kg).

2. Experimental

2.1. Materials and reagents

The azido and amino modified aptamers were purchased from Eurogentec (France). The binding site of the aptamers is identical with that reported in [31]. The aptamer sequences are show below

5′-GATCGGGTGTGGGTGGCGTAAAGGGAGCATCGGACA-3′), 5′-N_3
5′-GATCGGGTGTGGGTGGCGTAAAGGGAGCATCGGACA-3′), 5′-NH_2

All other chemicals, potassium ferricyanide ($K_3[Fe(CN)_6]$), potassium ferrocyanide ($K_4[Fe(CN)_6]$), sodium phosphate dibasic Na_2HPO_4, potassium phosphate monobasic KH_2PO_4, sulfuric acid (98%), ethanol (98%), and 4-((trimethylsilyl) ethynyl) aniline (TMSi-Eth-Ar-NH_2), 4-nitroaniline (p-NO_2-Ar-NH_2), sodium nitrite, ochratoxin A (OTA) (from *Aspergillus ochraceous*) and ochratoxin B (OTB) first dissolved in methanol and then diluted in binding buffer, Horseradish peroxidase (HRP, EC 1.11.1.7), tris(hydroxymethyl) aminomethane $(HOCH_2)_3$ CNH_2, Disodium ethylenediaminetetraacetate dihydrate EDTA disodium salt, EDTA-Na_2, (+)-sodium L-ascorbate, copper(II) sulfate pentahydrate and 3,3′,5,5′-tetramethylbenzidine (TMB) substrate, were all supplied by Sigma-Aldrich. Aptamer solutions prepared in binding buffer (BB) pH 7.4 containing 1 mM $MgCl_2$, 140 mM NaCl, 2.7 mM KCl, 0.1 mM Na_2HPO_4 and 1.8 mM KH_2PO_4 were used. The azido horseradish peroxidase (N_3-HRP) was synthesized according to the published procedure [27]. All solutions were prepared with deionized Milli-Q water (Millipore, Bedford, MA, USA).

2.2. Apparatus

The electrochemical measurements were carried out with an Autolab PGSTAT100 potentiostat/galvanostat (Eco Chemie, The Netherlands) with computerized control by GPES 4.9 and FRA software, connected to screen printed carbon electrode (SPCE), which comprises a working carbon electrode, printed from a carbon-based ink, a pseudo reference electrode made from a silver-based ink, and the auxiliary electrode from a carbon ink. The impedance spectra were recorded using a sinusoidal ac potential perturbation of 5 mV (rms), in the frequency range 10^4–0.5 Hz, superimposed on a dc potential of 0.095 V, and readings were taken at 20 discrete frequencies per decade. All measurements were performed in a solution of 1.0 mM ferri/ferrocyanide couple $[Fe(CN)6]^{4-/3-}$ in PBS, pH 7.3, as a background electrolyte.

2.3. Functionalization of SPCE surface with binary film of diazonium salts

The TMSi-Eth-Ar-N_2^+ ions were synthesized *in situ* by reaction of 2.0 mM TMSi-Eth-Ar-NH_2 and 2.0 mM sodium nitrate in 0.5 M HCl solution for 5 min. The electrochemical modification of SCPE with *in situ* generated TMSi-Eth-ArN_2^+ ions was performed by one potential cycling between 0.4 and −0.5 V. The modified SCPEs were subsequently treated with ethanol solution for 10 s to wash any physically adsorbed species. The p-NO_2-ArN_2^+ ions, obtained by the *in situ* reaction of 4-nitroaniline (2.0 mM) and sodium nitrate (2.0 mM) in 0.5 M HCl solution, were electrochemically immobilized onto TMSi-Eth-Ar-SPCE electrode. This protected surface TMSi-Eth-Ar-pNO_2-Ar-SPCE was treated with tetrabutylammonium fluoride (TBAF) to remove the TMSi group, and to obtain an ethynyl-modified surface.

2.4. Covalent immobilization of aptamer via click reaction

The immobilization of aptamer was performed by immersing the above ethynyl-modified SPCEs in azido-aptamer solution (0.5 μM) with sodium ascorbate (10.0 mM) and copper (II) sulfate pentahydrate (1.0 mM). The electrode with azido-aptamer solution was treated at −200 mV *vs.* pseudo ref. silver electrode for 5 min. The EDTA solution was used to remove the physically absorbed azide moieties and excess copper. For the electrochemical experiments, a 100 μL of OTA dissolved in BB was dropped onto the surface of the sensor, followed by incubation for 60 min in different concentrations of OTA (0.0–500 ng/L).

2.5. Regeneration of the impedimetric aptasensor

The electrodes were rinsed with distilled water after OTA incubation, and immediately used for electrochemical experiments. After each use, the electrodes were regenerated by washing with 100 μL of regeneration solution for 30 s The regenerating buffer was prepared according to a previously described protocol for regenerating the solid phase extraction column (methanol: eluting buffer (10.0 mM TRIS, 1.0 mM EDTA, pH 9.0) (20:80,v/v) [28].

2.6. Beer sample preparation

Samples were prepared following a protocol from a previous study [29]. In brief, the beer samples were spiked with the known concentration of stock solution of OTA. Afterwards, the spiked samples were cooled to 4 °C for 30 min to prevent rapid foam formation, which could cause sample overflow. Then the spiked samples were degassed by sonication for 1 h. The pH of beer was adjusted to 7.4. Finally, the spiked beer was passed through a filter (0.45 mm).

3. Results and discussion

3.1. SPCE surface modification chemistry

The cyclic voltammogram (CV) recorded at SPCE immersed in solution of the *in situ* generated protected TMSi-Eth-Ar-N_2^+ (Fig. 1A) shows a broad irreversible cathodic peak at 0.155 V (*vs.* pseudo Ag ref. electrode), assigned to the reduction of the diazonium species via one electron process, leads to protected TMSi-Eth-Ar radicals that couple to electrode surface with irreversible formation of a strongly bonded organic layer to the surface. During the second scan, the peak intensity dramatically decreases, consistent with the formation of a grafted layer on the electrode surface. Similarly, electrochemical reduction of the *in situ* generated *p*-NO_2-ArN_2^+ diazonium salt (Fig. 1B) at the protected TMSi-Eth-Ar-SPCE electrode shows an irreversible cathodic peak at −0.035 V (*vs.* pseudo Ag ref. electrode). A faster peak inhibition was observed, exhibiting very low or undetectable currents after the first scan. After *p*-NO_2-Ar grafting, it is possible to use CV in order to estimate the surface coverage of *p*-nitrophenyl groups at the surface. Fig. 1C shows CV obtained for TMSi-Eth-Ar-*p*-NO_2-Ar-SPCE as a working electrode in oxygen-free 0.1 M H_2SO_4 at 50 Vs−1. CV scans show the characteristic irreversible electroreduction peak arising from the reduction of nitrophenyl groups to aminophenyl groups; this is in agreement with previous reports of the electrochemistry of *p*-NO_2-Ar grafted layer [30]. An estimate of total surface coverage (Γ) can be evaluated from the charge passed (Q), by integrating the area under the voltammetric peaks at low scan rate, using the equation: $\Gamma = Q/nFA$; where n is the number of electrons transferred, F is Faraday's constant, and A is the electrode area. A surface concentration of $\Gamma = 4.02 \pm 0.93 \times 10^{-9}$ mol of active nitro groups electrografted to the electrode surface can be estimated. Immobilization of HRP via click chemistry was used to demonstrate the immobilization method. The detailed description along with supporting figures for HRP immobilization is provided in the Supplementary file 1.

3.2. Impedance studies of the modified electrode surface

The successful immobilization of each functionalized layer was confirmed through EIS measurements. Fig. 2 shows the Nyquist plots of impedance spectra after each surface modification step. On the basis of the charge transfer kinetics of the [Fe(CN)6]3−/4− redox probe, the Faradaic impedance spectra were modeled using the equivalent circuit approach of Randles (Fig. 2, inset). The circuit includes the commonly existing electrolyte resistance (*Rs*) and Warburg impedance (*Zw*) resulting from the diffusion of ions from the bulk of the electrolyte to the interface, double-layer capacitance (*Cd*), and the electron-transfer resistance (*R*et). The bare SPCE represented a very small circle at high frequencies, suggesting a very low electron transfer resistance to the redox probe dissolved in the electrolyte solution (curve a). When the 4-((trimethylsilyl) ethynyl) benzene was electrografted on the electrode to have ethynyl functional group on modified electrode, the *R*et increased to 250 kΩ, (curve b). When treated with ethanol, the *R*et decreased to 135 kΩ. When the reactive sites

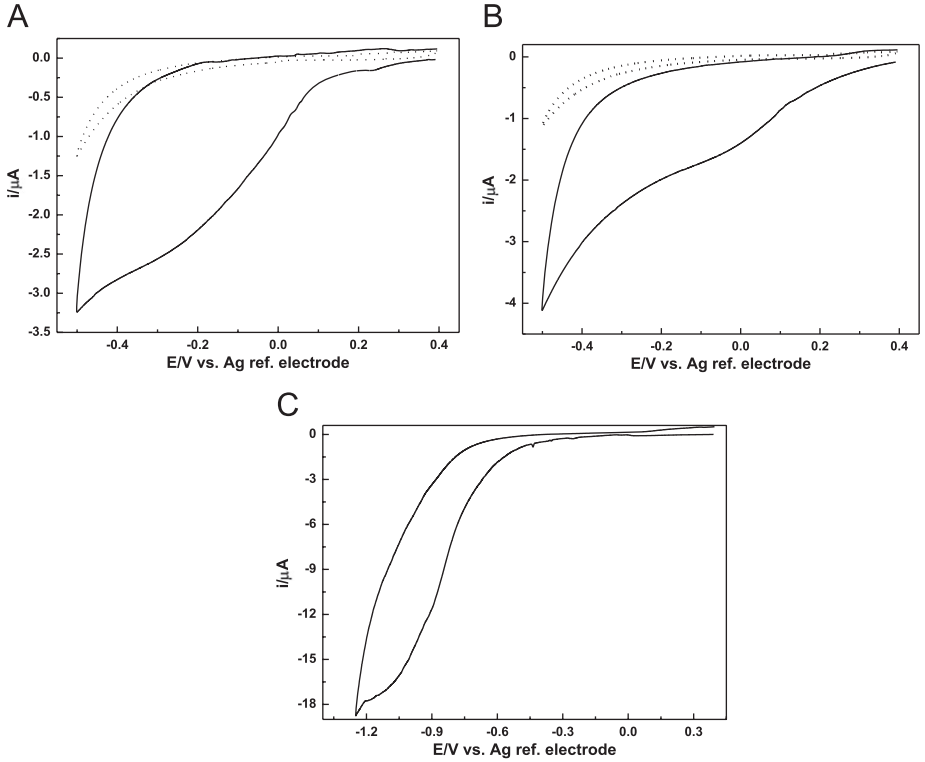

Fig. 1. (A) Cyclic voltammogram for the *in situ* generated 4-((trimethylsilyl)ethynyl)benzene diazonium TMSi-Eth-Ar-N_2^+; (B) *p*-nitrophenyl diazonium *p*-NO_2-ArN_2^+ on screen-printed carbon electrode from the diazotation mixture (2.0 mM $NaNO_2$, 2.0 mM corresponding aniline in 0.5 M HCl). Dotted lines: second scan, scan rate of 100 m Vs^{-1}; (C) cyclic voltammograms of modified screen-printed carbon electrode after post-functionalization with *p*-nitrophenyl in oxygen-free 0.1 M H_2SO_4, scan rate 100 m Vs^{-1}.

on the SPCE were blocked by the electroreduction of p-NO_2-ArN^{2+} ion that was used to cover the pinholes of the first layer for the design of uniform and compact modified electrode surface, the *R*et increased again to 525 kΩ. After deprotection, a significant decrease in blocking effect and a decrease in *R*et to 85 kΩ was observed. The immobilization of the aptamer induces an increase in the semi-circular diameter indicating an increase of the *R*et to 150 kΩ, due to the formation of a negatively charged layer which acts as an electrostatic barrier between the electrode surface and the $[Fe(CN)_6]4-/3-$ anions in the solution. The SPCE coverage rate, as $\theta = R_{et}$ (SPCE)/R_{et} (modified SPCE) was used to determine surface density at various modification steps. The obtained values were 9.6, 25 and 56.66% for TMSi-Eth-Ar-SPCE, H–Eth-Ar-p-NO_2-Ar-SPCE and aptamer modified electrode respectively. The blocking properties were also investigated by using CVs of a charged electroactive redox couple (ferri-/ferrocyanide), recorded after each treatment step. Detail discussion of CV results along with voltammograms on the different types of layers is provided in the Supplementary file 2.

3.3. Impedimetric aptasensor responses to target ochratoxin A

After the incubation of the aptamer-modified electrode in the regeneration buffer, a significant decrease in the blocking effect and a decrease in the *R*et to 70 kΩ were observed. It is likely that the regeneration buffer could affect the aptamers conformation. For OTA detection, aptamer modified electrodes after regeneration step were incubated with different concentrations of OTA solution for 1 h. The binding site of aptamer to OTA is not known yet. However, the work by Cruz-Aguado and Penner has demonstrated the high affinity of aptamer to OTA [31]. Moreover, numerous studies have shown that the aptamer affinity to OTA increases in the presence of metal ions [32,33]. To optimize the BB composition, experiments in the presence and absence of different mono/divalent cations were performed. The change in R_{et} was used to get the optimal conditions. It was observed that the addition of Ca^{2+} in BB containing $MgCl_2$ (1 mM), NaCl (140 mM) and KCl (2.7 mM) led to white precipitates and decreased the binding affinity of aptamer. Therefore, Ca^{2+} cations were not used in the BB for further experiments. The schematic presentation of the working principle of the aptasensor was shown in Scheme 1 (Scheme 1). The interaction between OTA and the aptamer layer was followed by an inhibition in the Faradaic response and an increase in the *R*et (Fig. 3A). The inhibition could be explained by the fact that the OTA binding to the surface-bound aptamer offers additional negative charges. The OTA molecule has a carboxyl and phenolic functional groups which give an OTA molecules with two anionic forms [12]. The existence of the two anionic states explains the blocking effect of the surface-bound OTA molecules for the electron transfer. The specific aptamer–OTA interaction induces an increase of the *R*et shown by larger semi-circular diameter proportional to the different tested concentrations. The calibration curve presented in Fig. 3B shows a non-linear dependence of the *R*et on the OTA concentration. It was found that the saturation of the electrode occurred at concentration values higher than 500 ng/L OTA. This phenomenon is caused by the binding of all the available active sites of the aptamer molecules on the electrode surface. Thus, the dynamic range of this impedimetric aptasensor ranges from 1.25 ng/L to 500 ng/L OTA; with a detection limit (LOD) of 0.25 ng/L ($S/N=3$). This is one of the lowest LOD reported for the electrochemical aptasensors of OTA [34].

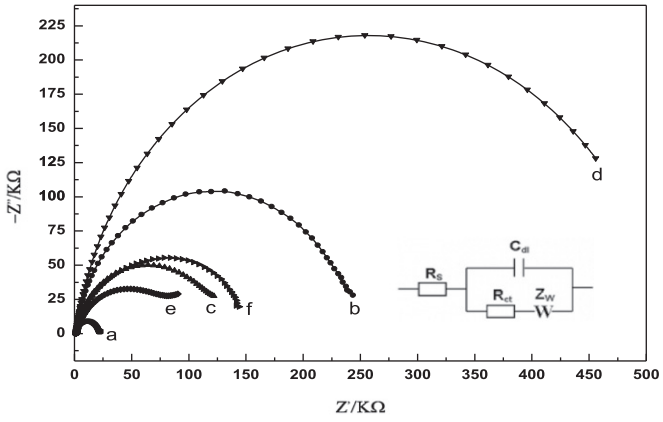

Fig. 2. Nyquist plots of 1.0 mM $[Fe(CN)_6]^{4-/3-}$ probe in PBS, pH 7.3, for (a) bare SPCE, (b) TMSi-Eth-Ar-SPCE, (c) after immersion of the protected TMSi-Eth-Ar-SPCE in ethanol, (d) H-Eth-Ar-p-NO_2-Ar-SPCE, (e) H-Eth-Ar-p-NO_2-Ar-SPCE after treatment with TBAF and (f) the aptamer modified electrode formed after dropping of 100 μL (0.5 μM) onto the H-Eth-Ar-p-NO_2-Ar-SPCE by applying a frequency range of 10^4–10^{-2} Hz, a bias potential of 0.095 V *vs.* pseudo Ag reference electrode and an ac amplitude of 5 mV. Inset: Randles equivalent circuit applied to fit the impedance spectroscopy.

3.4. Aptasensor regeneration

It is possible to regenerate the sensing interfaces with acid, alkali or salt to removed bound target molecules for the second measurement and onward. However, the regeneration of sensing interface is still a challenge for most of the existing aptasensors. In this work, a mild regeneration solution was used to renew the aptasensor. As shown in Fig. 4, when OTA binding electrode was regenerated, the R_{et} was recovered to the original value of newly prepared electrode, suggesting the reusability of the treated electrode (Fig. 4). When this treated electrode was incubated again with regenerating solution, the R_{et} value remained same as

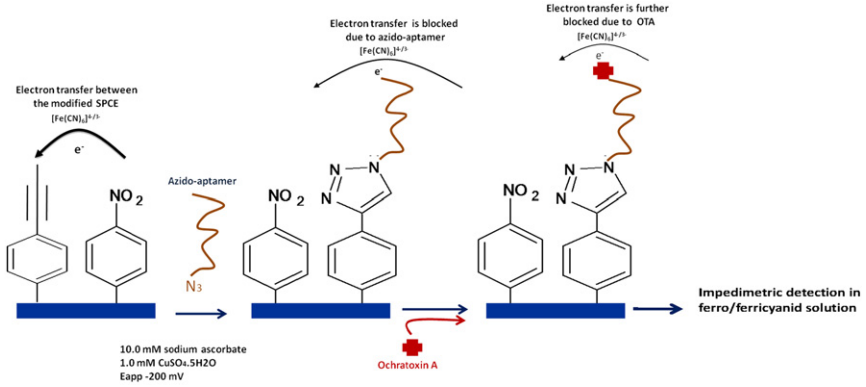

Scheme 1. Schematic presentation of the working principle of the developed impedimetric aptasensor.

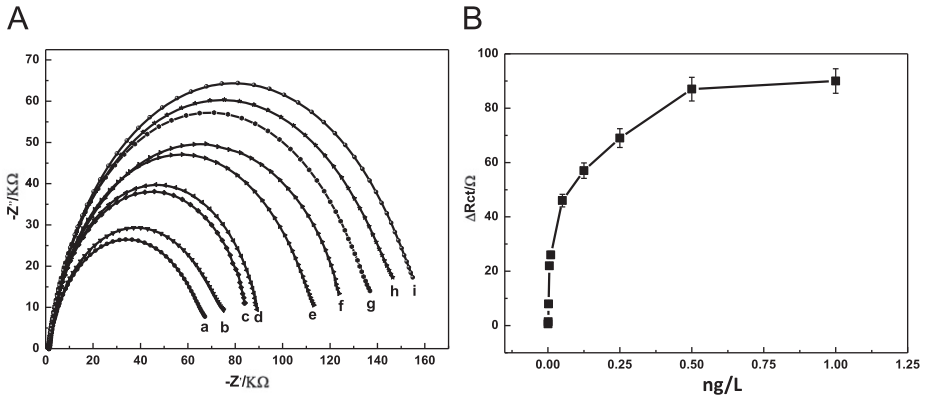

Fig. 3. (A) Nyquist plots after aptasensor incubation with different OTA concentrations (ng/L): (a) 0; (b) 1.25; (c) 2.50; (d) 5.00; (e) 10.00; (f) 50.00; (g) 125.00 (h) 250.00 and (i) 500 using 1.0 mM $[Fe(CN)_6]^{4-/3-}$ redox probe, a frequency range of 10^4–10^{-2} Hz, a bias potential of 0.095 V *vs.* pseudo Ag reference electrode and an ac amplitude of 5 mV; (B) inset: the calibration plot of the increase of the charge transfer resistance (R_{et}) with the OTA concentration for the aptasensor. Error bars represent means ± SD (n=5).

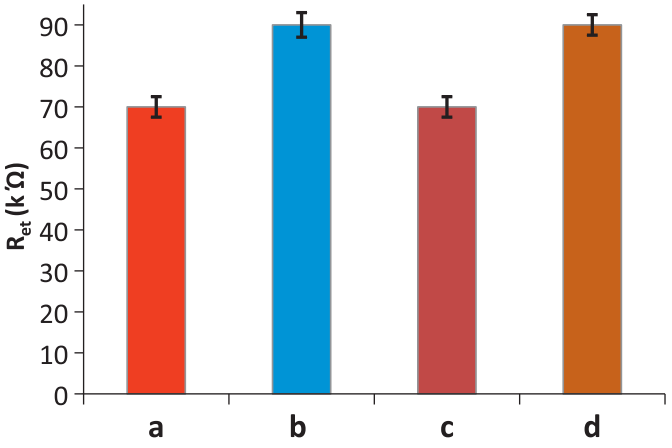

Fig. 4. OTA detection and regeneration of the sensing interface; (a) newly prepared electrode; (b) after being immersed in 5 ng/L of OTA; (c) regenerated electrode; (d) detection of 5 ng/L.

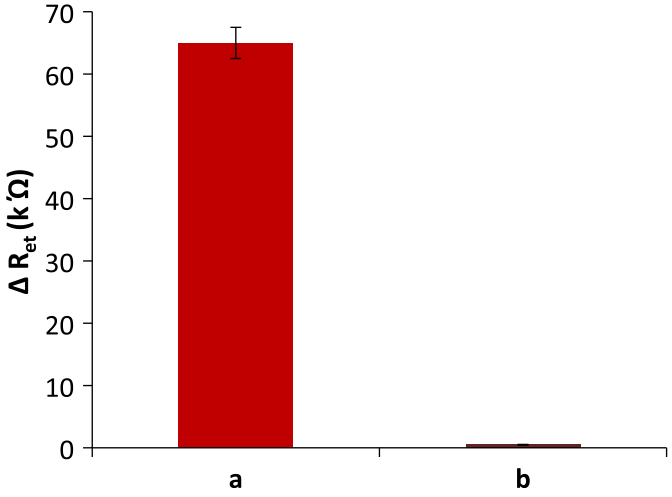

Fig. 5. Control experiments of the aptasensor; (a) 5 ng/L OTA; (b) 5 ng/L OTB; (c) blank binding buffer.

that of the first detection of OTA. Our results showed that the aptasensor regeneration at least up to 10 times had no significant effect on the sensor response for OTA determination. The developed aptasensor retained its EIS and CV response after a storage period of 10 days at 4 °C without loss of activity.

3.5. Specificity and reproducibility of the aptasensor

To investigate the non-specific adsorption of aptamer, amine-terminated aptamer (0.5 μM) was incubated on the ethynyl modified electrode. When ethynyl modified electrode was exposed to amino-terminated aptamer, the ΔR_{et} was 0.5 kΩ, and however, the ethynyl modified electrode incubation with azide-aptamer (0.5 μM) increased the ΔR_{et} to 65 kΩ (Supporting Fig. 1). The results indicated that the presence of aptamer on modified surface was due to click reaction, and not due to non-specific adsorption of aptamer. Similarly, in order to confirm that the change in impedance was based on the specific interaction between aptamer on electrode surface and OTA, and was not caused by non-specific adsorption of OTA, the ethynyl modified electrode was incubated with a sample of 5 ng/L of OTB as non-specific analyte and blank binding buffer. No significant difference in impedance measurements was observed before and after incubation with OTB and blank binding buffer (Fig. 5). These results confirmed that EIS changes observed with OTA were virtually due to specific OTA and aptamer complex formation. The reduced non-specific adsorption of OTA and aptamer could be contributed to the electrochemical grafting of binary layer of diazonium salts onto electrode surface, which resulted in the formation of a uniform and compact modified electrode surface. Our results showed that the design of robust binary film onto electrode could be an attractive alternative to generally used blocking solution to prevent non-specific signal in the construction of biosensors.

The reproducibility of the developed aptasensor was evaluated with interassay precision. The interassay precision was evaluated with same OTA concentration (5 ng/L) with five aptasensors independently prepared in the same experimental conditions. A relative standard deviation of 4.4% was calculated, indicating a very good reproducibility of the aptasensor. The good reproducibility results can be explained by the fact that the modified electrode surface provided appropriated and organized immobilization of aptamer, which resulted in improved repeatability of the aptasensor.

3.6. Application of the aptasensor to beer samples

To further study the potential application of the modified electrode, the detection of OTA in beer samples was performed. Assays were carried out by spiking the beer sample at two different levels of OTA (1.25 and 5 ng/L). Controls were achieved by adding the same amounts of OTA to binding buffer. As shown

Table 1
Analysis of beer samples spiked with known concentration of OTA.

Spiked OTA (ng/L)	A	B	RSD %
5	19.8	20	4.4
1.5	7.92	8	4.1

A, ΔR_{et} (k) for spiked beer samples; *B*, ΔR_{et} (k) for control-OTA diluted in binding buffer; RSD %, relative standard deviation percentage.

in Table 1, EIS responses to two concentration of OTA in beer sample exhibited same phenomena to those in blank buffer (Table 1). The results definitely showed analytical reliability and potential application of this aptasensor for reel sample.

3.7. Performance comparisons with other aptasensor reported in the literature for OTA detection

The performance of the developed impedimetric aptasensor was compared with the other reported aptasensors for OTA detection. It is noteworthy that the LOD (0.25 ng/L) obtained with our developed impedimetric apatasensor was many fold lower than the LOD (48.45–100 ng/L) of reported impedimetric apasensors for OTA detection [34,35]. The decreased LOD could be attributed to controlled aptamer immobilization via click chemistry, and to uniform and compact reactive surface for aptasensing in our aptasensor. The increased sensitivity and reduced non-specific signal for our aptasensor demonstrated the advantages of employing click chemistry and binary film grafting in the construction of aptasensors. Apart from impedimetric aptasensor, our developed aptasensor exhibited higher sensitivity than other labeled OTA aptasensors [33,36–40], without using any signal amplifying electroactive material. The performances of our developed aptasensor can be also advantageously compared with the immunoassays and immunosensor reported for OTA detection.

4. Conclusions

We have described a highly sensitive and reusable impedimetric aptasensor based on click chemistry. The immobilization via click chemistry not only improved the aptamer binding capacity but also magnified the response signal of the aptasensor. The reported work highlighted the interest of using two aryl diazonium salts on same electrode surface together with click chemistry in the development of aptasensor. In a word, the high-quality strategy for biomolecules immobilization opened the door to design simple, reusable and ultrasensitive aptasensor for many target molecules.

Acknowledgment

Akhtar Hayat is very grateful to Higher Education Commission of Pakistan for financial support. The authors acknowledge support through IMHOTEP Project.

Appendix A. Supporting information

Supplementary data associated with this article can be found in the online version at http://dx.doi.org/10.1016/j.talanta.2012.09.048.

References

[1] C. Tuerk, L. Gold, Science 249 (1990) 505–510.
[2] C.L.A. Hamula, J.W. Guthrie, H. Zhang, X.-F. Li, X.C. Le, TrAC, Trends Anal. Chem. 25 (2006) 681–691.
[3] C. Ding, Y. Ge, J.-M. Lin, Biosens. Bioelectron. 25 (2010) 1290–1294.
[4] K. Han, L. Chen, Z. Lin, G. Li, Electrochem. Commun. 11 (2009) 157–160.
[5] J.A. Hansen, J. Wang, A.N. Kawde, Y. Xiang, K.V. Gothelf, G. Collins, J. Am. Chem. Soc. 128 (2006) 2228–2229.
[6] M. Mir, I. Katakis, Mol. Biosyst. 3 (2007) 620–622.
[7] J. Yoshizumi, S. Kumamoto, M. Nakamura, K. Yamana, Analyst 133 (2008) 323–325.
[8] E.J. Cho, J.R. Collett, A.E. Szafranska, A.D. Ellington, Anal. Chim. Acta 564 (2006) 82–90.
[9] Z. Zhang, W. Yang, J. Wang, C. Yang, F. Yang, X. Yang, Talanta 78 (2009) 1240–1245.
[10] Y. Du, B. Li, H. Wei, Y. Wang, E. Wang, Anal. Chem. 80 (2008) 5110–5117.
[11] M. Shamsipur, M. Asgari, M.G. Maragheh, A.A. Moosavi-Movahedi, Bioelectrochemistry 83 (2012) 31–37.
[12] A.E. Radi, X. Munoz-Berbel, V. Lates, J.L. Marty, Biosens. Bioelectron. 24 (2009) 1888–1892.
[13] N. Meini, C. Farre, C. Chaix, K. Kherrat, S. Dzyadevych, N. Jaffrezic-Renault, Proc. Eng. 25 (2011) 1461–1464.
[14] Q. Shi, X. Chen, T. Lu, X. Jing, Biomaterials 29 (2008) 1118–1126.
[15] A.E. Daugaard, T.S. Hansen, N.B. Larsen, S. Hvilsted, Synth. Met. 161 (2011) 812–816.
[16] R. Huisgen, in: Padwa (Ed.), 1,3 Dipolar Cycloaddition Chemistry, 345, Wiley, New York, 1984, pp. 1–176.
[17] H.C. Kolb, M.G. Finn, K.B. Sharpless, Angew. Chem., Int. Ed. 40 (2001) 2004–2021.
[18] Q. Ran, R. Peng, C. Liang, S. Ye, Y. Xian, W. Zhang, L. Jin, Talanta 83 (2011) 1381–1385.
[19] H. Qi, C. Ling, R. Huang, X. Qiu, L. Shangguan, Q. Gao, C. Zhang, Electrochim. Acta 63 (2012) 76–82.
[20] N.K. Devaraj, J.P. Collman, QSAR Comb. Sci. 26 (2007) 1253–1260.
[21] Q. Ran, R. Peng, C. Liang, S. Ye, Y. Xian, W. Zhang, L. Jin, Anal. Chim. Acta 697 (2011) 27–31.
[22] A. Hayat, J.-L. Marty, A.-E. Radi, Electroanalysis 24 (2012) 1446–1452.
[23] A. Hayat, L. Barthelmebs, A. Sassolas, J.L. Marty, Talanta 85 (2011) 513–518.
[24] Y.R. Leroux, F. Hui, J.-M. Noël, C.m. Roux, A.J. Downard, P. Hapiot, Langmuir 27 (2011) 11222–11228.
[25] J. Beardall, J. Miller, Mycotoxin Res. 10 (1994) 21–40.
[26] L. Monaci, F. Palmisano, Anal. Bioanal. Chem. 378 (2004) 96–103.
[27] S.F.M. van Dongen, R.L.M. Teeuwen, M. Nallani, S.S. van Berkel, J.J.L.M. Cornelissen, R.J.M. Nolte, J.C.M. van Hest, Bioconjugate Chem. 20 (2008) 20–23.
[28] A. De Girolamo, M. McKeague, J.D. Miller, M.C. DeRosa, A. Visconti, Food Chem. 127 (2011) 1378–1384.
[29] A. Visconti, M. Pascale, G. Centonze, J. Chromatogr. A 888 (2000) 321–326.
[30] M. Delamar, G. Désarmot, O. Fagebaume, R. Hitmi, J. Pinsonc, J.M. Savéant, Carbon 35 (1997) 801–807.
[31] J.A. Cruz-Aguado, G. Penner, J. Agric. Food Chem. 56 (2008) 10456–10461.
[32] A. Rhouati, N. Paniel, Z. Meraihi, J.-L. Marty, Food Control 22 (2011) 1790–1796.
[33] L. Barthelmebs, A. Hayat, A.W. Limiadi, J.-L. Marty, T. Noguer, Sens. Actuat., B 156 (2011) 932–937.
[34] G. Castillo, I. Lamberti, L. Mosiello, T. Hianik, Electroanalysis 24 (2012) 512–520.
[35] N. Prabhakar, Z. Matharu, B.D. Malhotra, Biosens. Bioelectron. 26 (2011) 4006–4011.
[36] J. Chen, Z. Fang, J. Liu, L. Zeng, Food Control 25 (2012) 555–560.
[37] L. Barthelmebs, J. Jonca, A. Hayat, B. Prieto-Simon, J.-L. Marty, Food Control 22 (2011) 737–743.
[38] L. Sheng, J. Ren, Y. Miao, J. Wang, E. Wang, Biosens. Bioelectron. 26 (2011) 3494–3499.
[39] L. Bonel, J.C. Vidal, P. Duato, J.R. Castillo, Biosens. Bioelectron. 26 (2011) 3254–3259.
[40] H. Kuang, W. Chen, D. Xu, L. Xu, Y. Zhu, L. Liu, H. Chu, C. Peng, C. Xu, S. Zhu, Biosens. Bioelectron. 26 (2010) 710–716.